Synthesis and Optoelectrical Characterization of Novel Squaraine Dyes Derived from Benzothiophene and Benzofuran

G. Hanumantha Rao,[†,‡] Manish Pandey,[§] Kamatham Narayanaswamy,[†] Ravulakollu Srinivasa Rao,[†,‡] Shyam S. Pandey,*,[§] Shuzi Hayase,*,[§] and Surya Prakash Singh*,[†,‡]

[†]Polymers and Functional Materials Division, CSIR-Indian Institute of Chemical Technology, Uppal Road, Tarnaka, Hyderabad 500007, India

[‡]Academy of Scientific and Innovative Research (AcSIR), CSIR-Human Resource Development Centre, (CSIR-HRDC) Campus, Kamla Nehru Nagar, Ghaziabad, Uttar Pradesh 201002, India

[§]Graduate School of Life Science and Systems Engineering, Kyushu Institute of Technology, 2-4, Hibikino, Wakamatsu, Kitakyushu 808-0196, Japan

S *Supporting Information*

ABSTRACT: Synthesis and photophysical characterizations of two novel small molecules **SQ-BEN-THI** and **SQ-BEN-FUR** with D−A−D molecular structure consisting of squaraine as central unit and benzothiophene and benzofuran as end groups are being reported. Apart from very sharp and intense light absorption by these molecular sensitizers in near-infrared (NIR) wavelength region, their possibility as small molecular organic semiconductor was also explored after fabricating organic field-effect transistors (OFETs). Results obtained from photophysical, electrochemical, and quantum chemical studies were combined to elucidate the structural and optoelectronic properties. Electrical characterization pertaining to the charge-transport properties carried after OFET fabrication exhibited field-effect mobilities of 4.0×10^{-5} and 5.4×10^{-5} cm^2/(V s) for **SQ-BEN-THI** and **SQ-BEN-FUR,** respectively. After thermal annealing at 130 °C, the field-effect mobility was found to increase for both squaraine dyes. Relatively facile carrier transport in **SQ-BEN-FUR** compared to that of **SQ-BEN-THI** could be attributed to relatively higher backbone planarity as indicated from optimized molecular structure obtained after density functional theory calculations. This work may guide for further molecular design and synthesis of novel squaraine dyes for high-performance OFET applications.
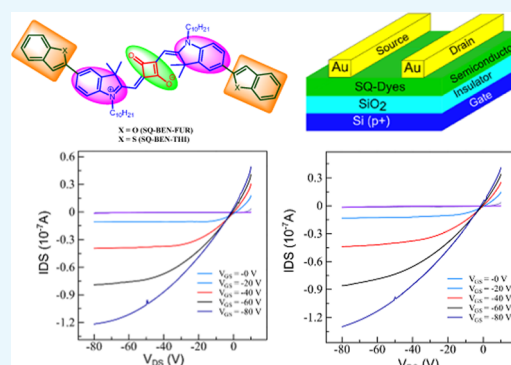
INTRODUCTION

Organic semiconductors are the main class of π-conjugated materials, which have been applied for next-generation optoelectronic applications particularly with regard to organic field-effect transistors (OFETs), organic light-emitting diodes (OLEDs), and organic photovoltaic cells.[1−5] Organic molecular semiconductors for OFETs have fascinated considerable interest pertaining to their widespread applications in sensors, high-region displays, radiofrequency identification tags, logic circuits with low production cost, and higher plasticity.[6−11] Many π-conjugated organic small molecules and polymers have been extensively developed and applied in OFETs as n-type, p-type, and ambipolar semiconducting materials such as pentacene,[12] fused thiophene derivatives,[13] diketopyrrolopyrroles,[14−17] merocyanines,[18,19] dinaphtho-thienothiophene,[20] naphthalene-diimides,[21−23] etc. with appreciable charge-carrier mobilities. Compared to polymeric materials, small molecules have captivated more observation in OFET applications because of their modular design allowing facile tuning of their electronic structure and energetics like highest occupied

molecular orbital (HOMO) and lowest unoccupied molecular orbital (LUMO) energy levels. They have many intrinsic advantages, i.e., well-elucidated molecular structures, molecular weights, high purity, and good charge-carrier mobility.[1−5] The performance of OFETs mainly depends on the structural characteristics of the active semiconducting material as well as the processing method employed during thin-film fabrication.[24] To reduce the fabrication cost for large-area manufacturing, implementation of solution process techniques like spin coating, blade coating, and inkjet printing are more favorable compared to vacuum deposition methods. However, such type of molecules should have facile solubility in organic solvents to employ solution-based processing along with relatively lower annealing temperatures to achieve stable and high device performance.

Squaraines come under polymethine class of dyes having zwitterionic structures. They possess an electron-deficient four-membered squaric acid ring at the center surrounded by two electron-donating moieties consisting of the donor—acceptor—donor (D−A−D) molecular framework. This class of organic molecules has been utilized for organic solar cells,[25] gas sensor,[26] biosensing,[27] nonlinear optics,[28] etc. due to intense and tunable absorption and emission from visible to near-infrared (NIR) wavelength region, but their application potential in the area of organic electronics has not been well explored. In 2007, Smits et al. reported solution-processable guaiazulenyl-derived squarylium dye[29] for NIR-sensitive light-emitting OFET applications with an ambipolar charge-carrier mobility of 10^{-4} cm^2/(V s). Later, Wöbkenberg et al. reported a squaraine dye for solution-processable single-layer organic phototransistors exhibiting ambipolar charge mobilities with balanced hole and electron transport.[30] A series of indole-based squaraine dyes were reported as air-stable semiconductors for OFETs with the highest carrier mobility of 4.8×10^{-3} cm^2/(V s) by Qiu group.[31] In 2014, Gsänger et al. reported[32] solution-processable squaraine dyes for OFET application exhibiting carrier mobility in the order of 10^{-4}–10^{-2} cm^2/(V s). Interestingly, there was a series of magnitude increase in the charge-carrier mobility when J-aggregate-assisted solution shearing method was used for thin-film processing emphasizing the importance processing technique on the film morphology and carrier transport. Squaraine dyes are structurally highly coplanar π-conjugated organic molecules, which have good charge-transport property through overlapping of π-orbitals and possess good film-forming ability. These properties of squaraine prompted us to design and synthesize two novel solution-processable squaraine-based small organic molecules like **SQ-BEN-THI** and **SQ-BEN-FUR** with D−A−D molecular structure consisting of benzothiophene and benzofuran, respectively, as π-conjugated donor end groups, as shown in Figure 1. We have

X=O (SQ-BEN-FUR)
X=S (SQ-BEN-THI)
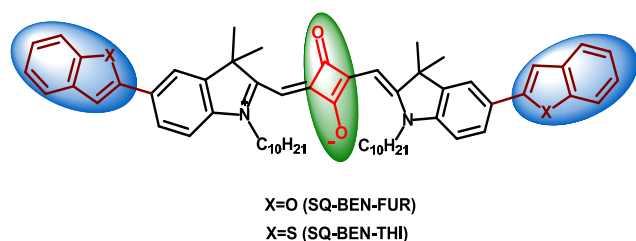
Figure 1. Molecular structure of newly designed squaraine dyes.

systematically studied the effect of heteroatom (oxygen and sulfur) substitution on their photophysical properties along with electrical characterization to explore their application as active semiconducting molecule for solution-processed OFETs. The synthetic route is represented in Scheme 1.

■ RESULTS AND DISCUSSION

Optical Characterization. Optical characterizations were performed using absorption and emission spectroscopies. Electronic absorption spectra for both of SQ-BEN-THI and SQ-BEN-FUR recorded in dichloromethane (DCM) solution and solid-state spin-coated thin films are shown in Figure 2. At the same time, corresponding optoelectronic data extracted from the optical characterizations are presented in Table 1. The maximum optical absorption (λ_{max}) in the solution

corresponding to lower energy bands was found at 672 and 674 nm for **SQ-BEN-THI** and **SQ-BEN-FUR**, respectively. These bands originated from the electronic transitions between the HOMO and LUMO and are associated with charge transfer (CT). Other higher-energy bands near 351 and 347 nm for **SQ-BEN-THI** and **SQ-BEN-FUR** are due to the π−π* electronic transitions, respectively. Both of the molecules show very high molar extinction coefficients of about 2×10^5 M^{-1} cm^{-1} in solution. A perusal of the solid-state electronic absorption spectra reveals that both of the molecules exhibit red-shifted and broadened spectral features compared to the solution state. This red shift of λ_{max} in the solid-state along with the spectral broadening is attributed to molecular aggregation due to enhanced intermolecular π−π interactions. Molecular aggregation is a commonly observed phenomenon in the π-extended planer molecular systems, and depending on the nature of molecules, there is formation of H-aggregation (blue-shifted) and J-aggregation[33,34] (red-shifted). It is very important to note that spectral broadening in the solid state extends toward the higher wavelength region compared to that in the solution state. This indicates the possibility of the development of J-aggregates in the solid state by molecular stacking. At the same time, thin-film absorption spectrum of the **SQ-BEN-FUR** appeared slightly red-shifted than **SQ-BEN-THI**, indicating the stronger molecular stacking compared to **SQ-BEN-THI**. This could be attributed to the presence of more electronegative O-atom of benzofuran ring of **SQ-BEN-FUR** compared to that of S-atom of benzothiophene in **SQ-BEN-THI**.

Fluorescence emission spectra of both the molecules in DCM solution, as shown in Figure 2b, exhibited emission maximum $\lambda_{max(em)}$ at 692 and 696 nm for **SQ-BEN-THI** and **SQ-BEN-FUR**, respectively. Difference between λ_{max} for electronic absorption and fluorescence emission spectrum is known as Stokes shift, which is considered to be originated from the energy losses due to vibrational relaxation, conformational changes, or molecular reorganization. It can be seen from the Table 1 that both of the molecules exhibit very small Stokes shift of only 20−22 nm, which suggests the molecular rigidity and conformational stability of the molecules in both the excited and ground states.[35] Optical band gap (E_g) is an important parameter especially of organic semiconductors and has been widely employed for the construction of energy band diagrams. Actually, the LUMO energy level for organic semiconductors has been determined by adding the energy corresponding to E_g to the HOMO energy level. E_g has been widely estimated from the absorption edge of the electronic absorption spectrum, which is good for the materials having a sharp and clear spectral onset. On the other hand, in many polymeric semiconductors where absorption spectrum is broad, determining the onset is prone to the errors. Intersection of absorption and emission spectrum has been defined as E_{o-o} and widely used to estimate E_g and LUMO, which has been used and shown in Table 1 for both the newly designed molecules.[36]

Electrochemical Characterization. Cyclic voltammetry (CV) has been widely used for the electrochemical characterizations pertaining to the determination of HOMO/LUMO and electrochemical band gap of organic semiconductors. CV was conducted for both molecules in DCM solution, and the three-electrode electrochemical cell consisted of platinum wire/coil as the counter electrode/working electrode and saturated calomel electrode (SCE) as the reference electrode.

Scheme 1. Synthetic Route Used To Prepare SQ-BEN-THI and SQ-BEN-FUR Dyes
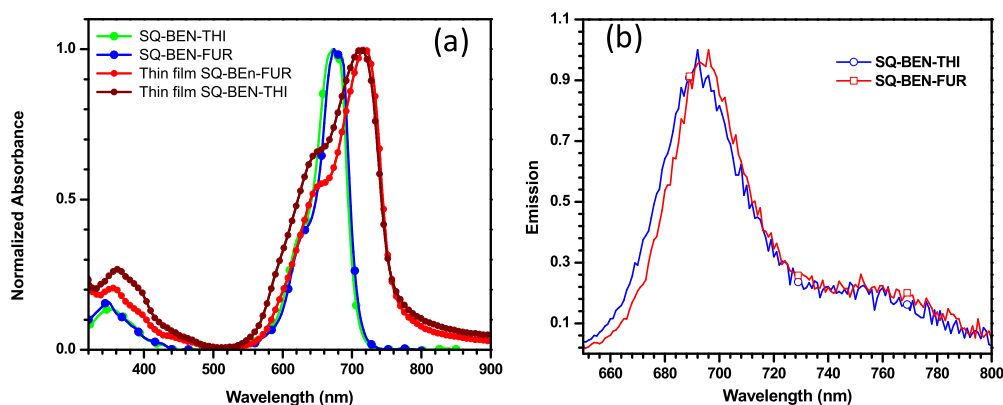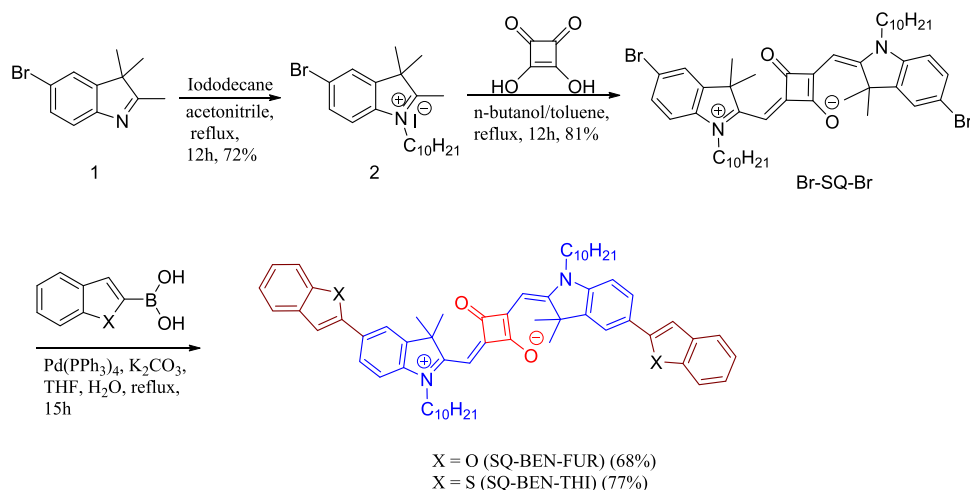
Figure 2. UV−vis absorption spectra of **SQ-BEN-THI** and **SQ-BEN-FUR** dyes recorded in DCM and in thin film (a) and their respective emission spectra in DCM solution (b).

The tetrabutylammonium perchlorate (0.1 M) and ferrocene/ferrocenium (Fc/Fc⁺) redox couple is used as an external standard. Cyclic voltammogram for both dye molecules **SQ-BEN-THI** and **SQ-BEN-FUR**, as shown in Figure 3, exhibited two reversible oxidation waves, and the potential for the first oxidation wave was used for the estimation of HOMO energy level. After running the CV for standard Fc/Fc⁺ redox couple, CV for the dyes was recoded under similar conditions and potentials were rescaled with respect to the Fc/Fc⁺ reference. Considering the well-accepted redox potential of Fc/Fc⁺ to be at +0.63 V versus NHE (−5.07 eV vs vacuum), the HOMO energy level was calculated from the first oxidation wave.[37] The value of this HOMO energy level estimated by CV for respective dye molecules was used to calculate the LUMO energy level by adding E_g (discussed in Section 3.1) and the calculated results are presented in Table 1.

Quantum Chemical Calculations. Molecular orbital (MO) calculations have been widely adopted for designing novel functional molecules to predict their energetics and electronic absorption spectra before performing the experiments to save experimental time. The geometries of **SQ-BEN-THI** and **SQ-BEN-FUR** dyes in isolated gaseous state were optimized by using (6-311G) basis set and linear spin density approximation (LSDA) exchange correlation function in Gaussian 09 programs.[38] The optimized geometry, HOMO and LUMO energy levels, with electronic distribution is

represented in Figure 4. The electron cloud in HOMO for both the dye molecules is mainly centralized at the central squaric acid core and slightly extended to the π-framework attached near to the core of the dye molecules.

However, the LUMO energy level is concerned with π* MO and the electron density is present over the squaric acid core and neighboring indole units along with a slight decrease of electron density at squaric acid core, indicating the possibility of intramolecular charge transfer upon photoexcitation. Energetics of the photofunctional molecules plays a dominant role for their utilization toward the optoelectronic application. Energy of HOMO calculated using 6-311G/LSDA predicts the HOMO energy values of −5.05 and −5.02 eV for both **SQ-BEN-THI** and **SQ-BEN-FUR**, respectively, which are in very good agreement with their respective experimental values determined from the CV and presented in Table 1. Considering the experimental values of HOMO of −5.12 and −5.11 eV (Table 1) for **SQ-BEN-THI** and **SQ-BEN-FUR** along with most commonly used value for work function of −5.10 eV for Au, it seems that Au can function as an Ohmic contact (source−drain (S−D)) material for fabricating electronic devices like field-effect transistors.[39]

To better understand the electronic transition, oscillator strength and molar extinction coefficients of both the dyes, the time-dependent density functional theory (TD-DFT) method was performed using similar exchange correlation functional

Table 1. Optical and Electrochemical Parameters for Symmetrical Squaraine Dyes

dye	$\lambda_{max\,(abs)}$,[a] nm ($\varepsilon_{max} \times 10^5$, M^{-1} cm^{-1})	$\lambda_{max(em)}$,[b] nm	$\lambda_{max(abs)}$,[c] nm, thin film	E_{OX} (V) vs Fc/Fc$^+$	E_{0-0}[d] eV	Stokes shift,[e] nm	HOMO, eV	LUMO, eV
SQ-BEN-THI	672 (2.07)	692	713	0.05	1.81	20	−5.12	−3.31
SQ-BEN-FUR	674 (2.08)	696	718	0.04	1.79	22	−5.11	−3.32

[a]UV−vis absorption maxima of dyes in the dichloromethane solution. [b]Fluorescence emission maxima of dyes in the dichloromethane solution. [c]Electronic absorption maxima of dyes on thin film. [d]Calculated from intersection of the absorption and emission spectra. [e]Calculated from difference between absorption maximum and emission maximum. Redox potential of ferrocene/ferrocenium (Fc/Fc$^+$) has been considered to be +0.63 V vs normal hydrogen electrode (NHE).
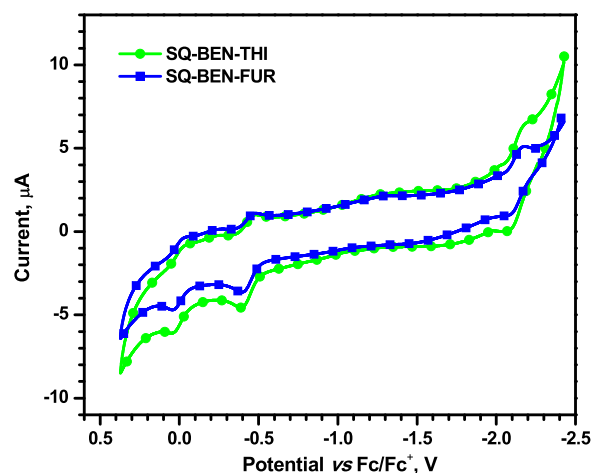
Figure 3. Cyclic voltammogram for dye molecules **SQ-BEN-THI** and **SQ-BEN-FUR** recorded in DCM solution.

and basis set in Gaussian 09 programs after optimization of geometry. Figure 5 represents the calculated vertical excitation energies from the ground state to the lowest singlet excited states and theoretical electronic absorption. Theoretical absorption spectra show the intense band centered at 659 and 661 nm having oscillator strengths of 2.055 and 2.050 for **SQ-BEN-THI** and **SQ-BEN-FUR**, respectively, mainly attributed to the $\pi-\pi^*$ electronic transition from the HOMO−LUMO energy level. A perusal of this calculated λ_{max} of about 660 nm for both the squaraine dyes reveals that calculated λ_{max} is slightly hypsochromically shifted in comparison to experimental values (about 672 and 674 nm) as shown in Table 1. This very small difference (12−14 nm (about 0.01 eV)) between the experimentally observed values λ_{max} and theoretical calculation ones indicates that this is the potentiality methodology for the theoretical calculation of absorption spectra.

Electrical Characterization. Results pertaining to the HOMO energy values for both the newly designed symmetrical squaraine dye molecules obtained by combined theoretical and experimental approaches and optical E_g, as shown in Table 1, indicate that these molecules may behave as moderate-band-gap organic semiconductors. To explore this possibility, electrical characterization experiments were performed by fabricating the OFETs in the bottom gate top contact device architecture and utilizing both these dyes as organic semiconductor. Schematic representation of the device architecture used in this work is shown in the Figure 6a.

Results obtained from the $I-V$ characteristics of the OFETs based on both **SQ-BEN-THI** and **SQ-BEN-FUR** are shown in Figure 6b,c. It can be clearly seen that both the OFETs operate after application of negative gate bias reflecting p-type charge-transport behavior with relatively larger output current observed in the case of OFETs based on **SQ-BEN-FUR**. Transfer characteristics of the fabricated OFETs based on both the dye molecules are shown in Figure 7a,b. Device parameters such as field-effect mobility (μ), on/off ratio, and threshold voltage (V_{th}) were extracted from the transfer curves in the saturation regime of the transfer properties using eq 1 along with summarization of the extracted results in Table 2.

$$I_{DS} = \frac{W}{2L}\mu C_i (V_{GS} - V_{th})^2 \qquad (1)$$
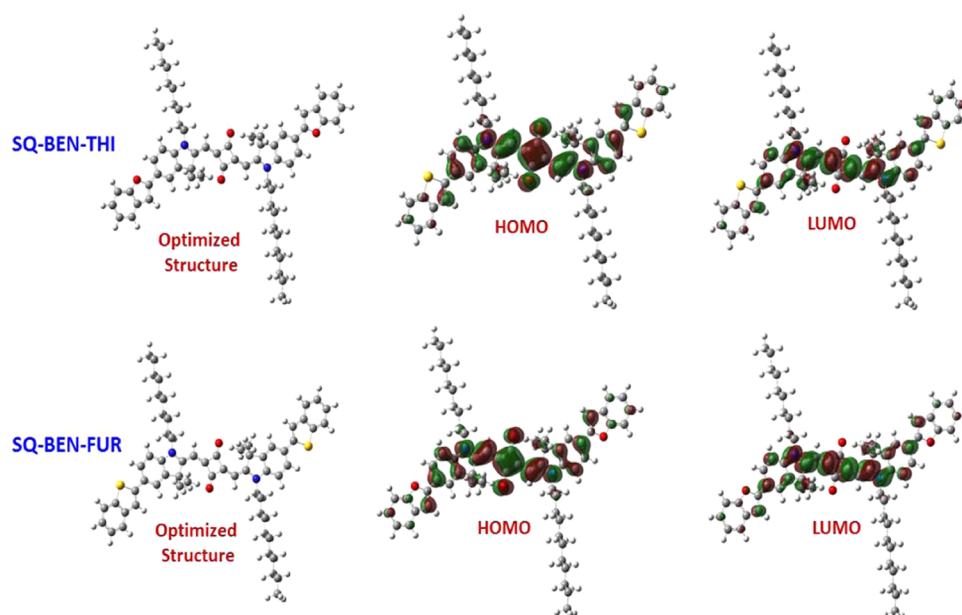
Figure 4. Computational result of the optimized structure and electron density distribution in HOMO and LUMO of the newly designed squaraine dyes utilized in this work.
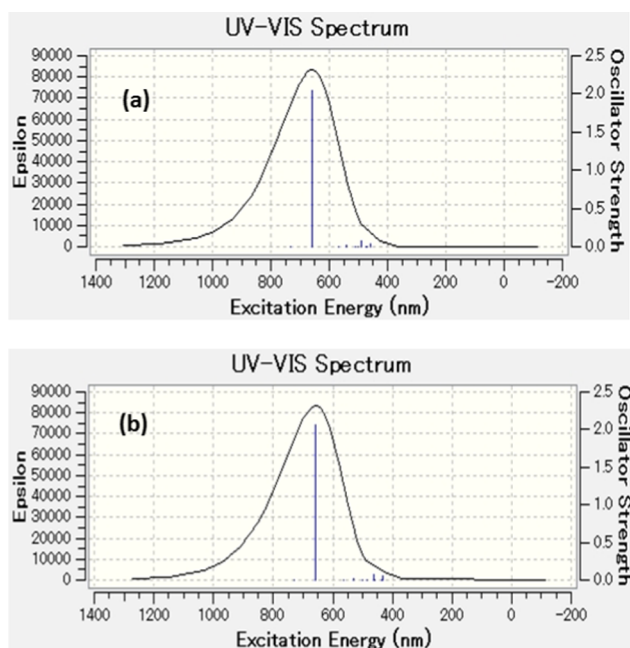
Figure 5. Theoretical absorption spectra for **SQ-BEN-THI** (a) and **SQ-BEN-FUR** (b) using TD-DFT under 6-311G/LSDA in isolated gaseous state.

Field-effect mobilities of 4.0×10^{-5} and 5.4×10^{-5} cm²/(V s) were found to be for the **SQ-BEN-THI** and **SQ-BEN-FUR** molecules, respectively. This slightly higher observed mobility for the OFET-based on **SQ-BEN-FUR** has been confirmed for multiple devices using this dye molecule. As can be seen from Figure 7, annealing the films for 10 min led to a slight increase in the charge-carrier mobility; however, there was no significant trend observed for the on/off ratio of the OFETs.

■ **CONCLUSIONS**

Synthesis and photophysical characterizations for two novel and near-infrared sensitive small molecules, namely, **SQ-BEN-**

THI and **SQ-BEN-FUR**, with D−A−D molecular structure consisting of squaraine as central unit, benzothiophene, and benzofuran as end groups have been reported. Photophysical, electrochemical, and quantum chemical calculation results were combined to describe the structural, optical, and electronic properties of two newly designed squaraine dyes. Electrical characterization has been made using these molecules as active organic semiconductor after FET fabrication in bottom gate top contact device architecture. OFETs thus fabricated showed field-effect mobilities of 4.0×10^{-5} and 5.4×10^{-5} cm²/(V s) for **SQ-BEN-THI** and **SQ-BEN-FUR**, respectively. After thermal annealing at 130 °C, the field-effect mobility slightly increased up to 7.4×10^{-5} cm²/(V s) for **SQ-BEN-FUR** and 5.0×10^{-5} for **SQ-BEN-THI**. We have systematically studied the effect of heteroatom (oxygen and sulfur) substitution on the optical, electrochemical, and electrical properties. Considering all of the results, we assume that more efforts to design and synthesize new squaraine-based p-type semiconductors are extremely pivotal to further pursue their scope as carriers and structure−property connectivity.

■ **EXPERIMENTAL SECTION**

Materials and Method. All starting materials, benzo[*b*]-thien-2-ylboronic acid, 2-benzofuranylboronic acid, iodode-cane, and squaric acid, were purchased from Alfa-Aesar, Aldrich. Final synthesized dyes were characterized by nuclear magnetic resonance (NMR) and high-resolution mass spectroscopy (HRMS) for structural verification. ^{1}H (400, 300, and 500 MHz) and ^{13}C (150 MHz) NMR spectra were recorded using Avance-400, AMX2-500, and Avance ACP-300 NMR spectrometers; tetramethylsilane (TMS) is used as an internal standard. HRMS images were obtained on a Shimadzu LCMS-2010 EV model equipped with an ESI probe. Absorption spectra in dichloromethane (DCM) solution and solid state (spin-coated thin film on glass) were recorded on a UV−visible−NIR spectrophotometer (model and make). Fluorescence emission spectra of dyes were recorded in DCM solution using a fluorescence spectrometer (model and make).
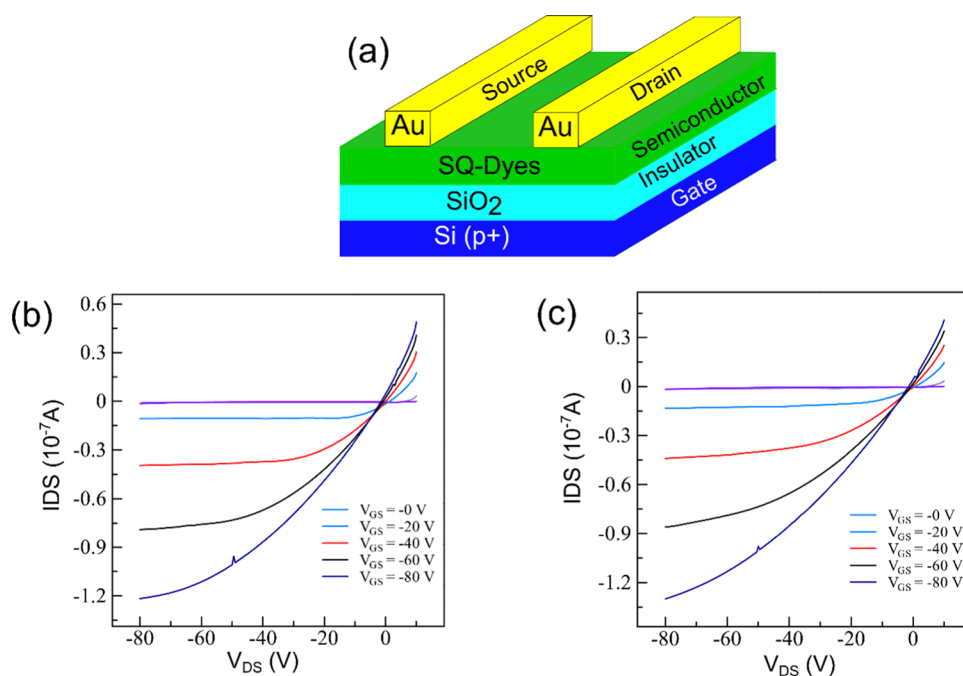
Figure 6. (a) Device structure of fabricated bottom gate top contact OFETs and output characteristics for OFETs utilizing (b) **SQ-BEN-THI** and (c) **SQ-BEN-FUR** as active semiconducting material.
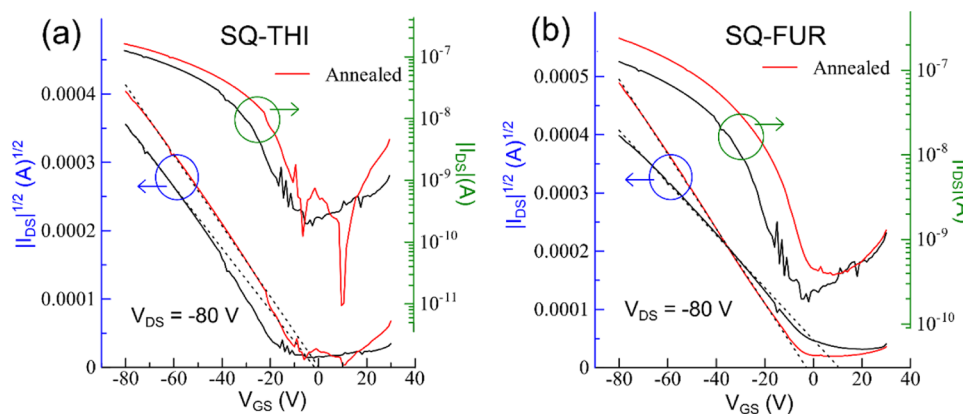
Figure 7. Transfer characteristics for the OFETS fabricated using spin-coated films of **SQ-BEN-THI** (a) and **SQ-BEN-FUR** (b).

Table 2. Optical and Electrochemical Parameters for Symmetrical Squaraine[a]

dye molecules	thermal treatment[a,b]	mobility (cm^2/(V s))	on/off ratio (×10^3)	threshold voltage (V)
SQ-BEN-THI	b	4.0×10^{-5}	6.0×10^2	2
	a	5.0×10^{-5}	1.0×10^3	0
SQ-BEN-FUR	b	5.4×10^{-5}	6.0×10^3	−3
	a	7.4×10^{-5}	6.0×10^3	−2

[a]a and b represent the results extracted for devices utilizing dyes after and before annealing of the dyes, respectively.

Cyclic voltammetry (CV) for electrochemical characterization was conducted on a CH Instruments three-electrode system consisting of Pt working electrode, Ag/AgCl reference electrode, counter electrodes. CV of the dyes was performed in DCM solution containing 2 mM respective dyes and 0.1 M tetrabutylammonium perchlorate electrolyte at a scan rate of 100 mV s^{-1}. Optimized geometries of final dyes along with the HOMO, LUMO, and absorption spectra were calculated using TD-DFT without any symmetry restriction using linear spin density approximation as optimized functional for squaraine

dyes and 6-311G basis set as executed in Gaussian 09 program package.[40−42]

Synthetic Procedure. Newly designed symmetrical squaraine dyes with molecular structure displayed in Figure 1 were synthesized by Pd-assisted Suzuki cross-coupling between the dye intermediate (Z)-4-((5-bromo-1-decyl-3,3-dimethyl-3H-indol-1-ium-2-yl)methylene)-2-((E)-(5-bromo-1-decyl-3,3-dimethylindolin-2-ylidene)methyl)-3-oxocyclobut-1-enolate (Br-SQ-Br) and benzo[b]thien-2-ylboronic acid and 2-benzofuranylboronic acid, as shown schematically in Scheme 1. The dye intermediate (Z)-4-((5-bromo-1-decyl-3,3-dimethyl-

3H-indol-1-ium-2-yl)methylene)-2-((E)-(5-bromo-1-decyl-3,3-dimethylindolin-2-ylidene)methyl)-3-oxocyclobut-1-enolate (Br-SQ-Br) was synthesized via the reported procedure.[43]

(Z)-4-((5-(Benzo[b]thiphen-2-yl)-1-decyl-3,3-dimethyl-3H-indol-1-ium-2-yl)methylene)-2-((E)-(5-(benzo[b]thiophen-2-yl)-1-decyl-3,3-dimethylindolin-2-ylidene)methyl)-3-oxocyclobut-1-enolate (SQ-BEN-THI). A mixture of Br-SQ-Br (300 mg, 0.35 mmol) and benzo[b]thien-2-ylboronic acid (160 mg, 0.89 mmol) was added to 10 mL of THF solution in a round-bottom flask, and then 2 mL of 2 M Na_2CO_3, $Pd(PPh_3)_4$ (12 mg, 0.01 mmol) was added to the reaction mixture and degassed for about 15 min. The reaction was carried out at 60 °C for 15 h under nitrogen atmosphere. The solvent was removed under vacuum and then the residue was taken up with dichloromethane (DCM) and washed with water. The organic layer was dried over anhydrous Mg_2SO_4. The filtrate was concentrated under vacuum and purified by column chromatography (eluent: methanol/DCM 1:99) to furnish **SQ-BEN-THI** as a blue solid. Yield: 260 mg (77%). Fourier transform infrared (FTIR) (KBr, cm^{-1}) $\tilde{v}$ = 2922 (ν_{C-H}), 1593 ($\nu_{C=O}$) cm^{-1}. ^{1}H NMR (300 MHz, CDCl$_3$, TMS): δ = 7.82 (d, J = 8 Hz, 2H), 7.77 (d, J = 8 Hz, 2H), 7.64−7.67 (m, 4H), 7.54 (s, 2H), 7.25−7.37 (m, 4H), 7.01 (d, J = 8.5 Hz, 2H), 6.01 (s, 2H), 4.00 (bs, 4H), 1.86 (s, 12H), 1.41−1.47 (m, 4H), 1.35−1.37 (m, 4H), 1.26−1.31 (m, 22H), 0.88 (t, J = 7.5, 6H) ppm. ^{13}C NMR (125 MHz, CDCl$_3$): δ = 182.3, 179.6, 169.5, 143.7, 143.0, 142.5, 140.7, 139.2, 130.1, 126.4, 124.6, 124.2, 123.4, 122.1, 120.2, 119.0, 109.6, 87.3, 49.2, 43.9, 31.8, 29.4, 29.3, 29.2, 27.15, 27.1, 27.0, 22.6, 14.0 ppm. HRMS m/z: calculated for $C_{62}H_{72}N_2O_2S_2$, [M + H]$^+$ m/z 941.3773 and found 941.5109.

(Z)-4-((5-(Benzofuran-2-yl)-1-decyl-3,3-dimethyl-3H-indol-1-ium-2-yl)methylene)-2-((E)-(5-(benzofuran-2-yl)-1-decyl-3,3-dimethylindolin-2-ylidene)methyl)-3-oxocyclobut-1-enolate (SQ-BEN-FUR). Synthetic procedure is the same as in **SQ-BEN-THI**. Br-SQ-Br (210 mg, 0.25 mmol), 2-benzofuranylboronic acid (121 mg, 0.75 mmol). Yield: 155 mg (68%). FTIR (KBr, cm^{-1}) $\tilde{v}$ = 2921 (ν_{C-H}), 1601 ($\nu_{C=O}$) cm^{-1}. ^{1}H NMR (400 MHz, CDCl$_3$, TMS): δ = 7.81−7.84 (m, 4H), 7.58 (d, J = 8 Hz, 2H), 7.54 (d, J = 8 Hz, 2H), 7.27−7.31 (m, 2H), 7.22−7.25 (m, 2H), 7.01−7.05 (m, 4H), 6.02 (s, 2H), 4.00 (bs, 4H), 1.87 (s, 12H), 1.41−1.48 (m, 5H), 1.22−1.41 (m, 27H), 0.87 (t, 6H) ppm. ^{13}C NMR (100 MHz, CDCl$_3$): δ = 201.8, 199.1, 189.0, 175.1, 174.3, 162.4, 162.2, 148.8, 145.7, 144.3, 143.6, 142.5, 140.2, 138.3, 130.5, 129.1, 120.2, 106.8, 68.7, 63.4, 51.3, 48.9, 48.8, 48.7, 46.6, 46.5, 42.1, 33.5 ppm. HRMS m/z: calculated for $C_{62}H_{72}N_2O_4$, [M + H]$^+$ m/z 909.2461, found 909.5565.

Device Fabrication. A highly p-doped silicon possessing 300 nm of SiO_2 as gate dielectric insulator with a gate capacitance (C_i) of 10 nF/cm^2 was used for fabricating OFETs. A 2% (w/w) solution of both of the dyes was prepared in dehydrated chloroform (Sigma-Aldrich) and spin-coated on SiO_2 at 3000 rpm for 30 s. Annealing was performed under argon atmosphere at 130 °C for 10 min prior to electrode deposition. Gold (Au) was utilized for source (S) and drain (D) electrodes and thermally deposited on the spin-coated dye layer having a thickness of 50 nm at a base pressure of 10^{-6} Torr using Nickel shadow mask. Channel length (L) and width (W) of the mask were 20 μm and 2 mm, respectively. All OTFTs were electrically isolated prior to the characterization by removing the semiconductor film around the device by cotton bud dipped in chloroform. Drain current−drain voltage

($I_{DS}-V_{DS}$) as well as the drain current gate voltage ($I_{DS}-V_{GS}$) characteristics were measured using a computer-controlled two-channel electrometer (Keithley 2612). Device parameters were extracted from the transfer curves.

■ ASSOCIATED CONTENT

⑤ Supporting Information

The Supporting Information is available free of charge on the ACS Publications website at DOI: 10.1021/acsomega.8b01240.

Detailed description regarding ^{1}H NMR, ^{13}C NMR, and HRMS (PDF)

■ AUTHOR INFORMATION

Corresponding Authors
*E-mail: shyam@life.kyutech.ac.jp (S.S.P.).
*E-mail: hayase@life.kyutech.ac.jp (S.H.).
*E-mail: spsingh@iict.res.in (S.P.S.).
ORCID ⊙
Manish Pandey: 0000-0003-0963-8097
Shyam S. Pandey: 0000-0001-8102-1003
Surya Prakash Singh: 0000-0001-5670-7329
Notes
The authors declare no competing financial interest.

■ ACKNOWLEDGMENTS

■ REFERENCES

(1) Zhang, L.; Colella, N. S.; Cherniawski, B. P.; Mannsfeld, S. C. B.; Briseno, A. L. Oligothiophene Semiconductors: Synthesis, Characterization, and Applications for Organic Devices. *ACS Appl. Mater. Interfaces* **2014**, *6*, 5327−5343.

(2) Caironi, M.; Anthopoulos, T. D.; Noh, Y.-Y.; Zaumseil, J. Organic and Hybrid Materials for Flexible Electronics. *Adv. Mater.* **2013**, *25*, 4208−4209.

(3) Usta, H.; Facchetti, A.; Marks, T. J. n-Channel Semiconductor Materials Design for Organic Complementary Circuits. *Acc. Chem. Res.* **2011**, *44*, 501−510.

(4) Facchetti, A. Semiconductors for Organic Transistors. *Mater. Today* **2007**, *10*, 28−37.

(5) Vercelli, B.; Pasini, M.; et al. Phenyl- and Thienyl-Ended Symmetric Azomethines and Azines as Model Compounds for n-Channel Organic Field-Effect Transistors: An Electrochemical and Computational Study. *J. Phys. Chem. C* **2014**, *118*, 3984−3993.

(6) Sirringhaus, H.; Tessler, N.; Friend, R. H. Integrated Optoelectronic Devices Based on Conjugated Polymers. *Science* **1998**, *280*, 1741−1744.

(7) Kagan, C. R.; Mitzi, D. B.; Dimitrakopoulos, C. D. Organic-Inorganic Hybrid Materials as Semiconducting Channels in Thin-Film Field-Effect Transistors. *Science* **1999**, *286*, 945−947.

(8) Crone, B.; Dodabalapur, A.; Gelperin, A.; Torsi, L.; Katz, L. H. E.; Lovinger, J.; Bao, Z. Electronic Sensing of Vapors with Organic Transistors. *Appl. Phys. Lett.* **2001**, *78*, 2229−2231.

(9) Cicoira, F.; Santato, C. Organic Light Emitting Field Effect Transistors: Advances and Perspectives. *Adv. Funct. Mater.* **2007**, *17*, 3421−3434.

(10) Sung, C. F.; Kekuda, D.; Chu, L. F.; Lee, Y. Z.; Chen, F. C.; Wu, M. C.; Chu, C. W. Flexible Fullerene Field-Effect Transistors Fabricated Through Solution Processing. *Adv. Mater.* **2009**, *21*, 4845−4849.

(11) Sirringhaus, H. Device Physics of Solution-Processed Organic Field-Effect Transistors. *Adv. Mater.* **2005**, *17*, 2411−2425.

(12) Lin, Y.-Y.; Gundlach, D. J.; Nelson, S. F.; Jackson, T. N. Stacked Pentacene Layer Organic Thin-Film Transistors with Improved Characteristics. *IEEE Electron Device Lett.* **1997**, *18*, 606−608.

(13) Wu, W.; Liu, Y.; Zhu, D. π-Conjugated Molecules with Fused Rings for Organic Field-Effect Transistors: Design, Synthesis and Applications. *Chem. Soc. Rev.* **2010**, *39*, 1489−1502.

(14) Zhang, Y.; Kim, C.; Lin, J.; Nguyen, T.-Q. Solution-Processed Ambipolar Field-Effect Transistor Based on Diketopyrrolopyrrole Functionalized with Benzothiadiazole. *Adv. Funct. Mater.* **2012**, *22*, 97−105.

(15) Qiao, Y.; Guo, Y.; Yu, C.; Zhang, F.; Xu, W.; Liu, Y.; Zhu, D. Diketopyrrolopyrrole-Containing Quinoidal Small Molecules for High-Performance, Air-Stable, and Solution-Processable n-Channel Organic Field-Effect Transistors. *J. Am. Chem. Soc.* **2012**, *134*, 4084−4087.

(16) Suraru, S.-L.; Zschieschang, U.; Klauk, H.; Würthner, F. Diketopyrrolopyrrole as a p-Channel Organic Semiconductor for High Performance OTFTs. *Chem. Commun.* **2011**, *47*, 1767−1769.

(17) Yoon, W. S.; Park, S. K.; Cho, I.; Oh, J.-A.; Kim, J. H.; Park, S. Y. High-Mobility n-Type Organic Transistors Based on a Crystallized Diketopyrrolopyrrole Derivative. *Adv. Funct. Mater.* **2013**, *23*, 3519−3524.

(18) Bürckstümmer, H.; Tulyakova, E. V.; Deppisch, M.; Lenze, M. R.; Kronenberg, N. M.; Gsänger, M.; Stolte, M.; Meerholz, K.; Würthner, F. Efficient Solution-Processed Bulk Heterojunction Solar Cells by Antiparallel Supramolecular Arrangement of Dipolar Donor−Acceptor Dyes. *Angew. Chem., Int. Ed.* **2011**, *50*, 11628−11632.

(19) Huang, L.; Stolte, M.; Bürckstümmer, H.; Würthner, F. High-Performance Organic Thin-Film Transistor Based on a Dipolar Organic Semiconductor. *Adv. Mater.* **2012**, *24*, 5750−5754.

(20) Yamamoto, T.; Takimiya, K. Facile Synthesis of Highly π-Extended Heteroarenes, Dinaphtho[2,3-b:2′,3′-f]chalcogenopheno-[3,2-b]chalcogenophenes, and Their Application to Field-Effect Transistors. *J. Am. Chem. Soc.* **2007**, *129*, 2224−2225.

(21) Guo, X.; Kim, F. S.; Seger, M. J.; Jenekhe, S. A.; Watson, M. D. Naphthalene Diimide-Based Polymer Semiconductors: Synthesis, Structure−Property Correlations, and n-Channel and Ambipolar Field-Effect Transistors. *Chem. Mater.* **2012**, *24*, 1434−1442.

(22) Kim, R.; Amegadze, P. S. K.; Kang, I.; Yun, H.-J.; Noh, Y.-Y.; Kwon, S.-K.; Kim, Y.-H. High-Mobility Air-Stable Naphthalene Diimide-Based Copolymer Containing Extended π-Conjugation for n-Channel Organic Field Effect Transistors. *Adv. Funct. Mater.* **2013**, *23*, 5719−5727.

(23) Würthner, F.; Stolte, M. Naphthalene and Perylene Diimides for Organic Transistors. *Chem. Commun.* **2011**, *47*, 5109−5115.

(24) Zhang, C.; Zang, Y.; Gann, E.; McNeill, C. R.; Zhu, X.; Di, C.-A.; Zhu, D. Two-Dimensional π-Expanded Quinoidal Terthiophenes Terminated with Dicyanomethylenes as n-Type Semiconductors for High-Performance Organic Thin-Film Transistors. *J. Am. Chem. Soc.* **2014**, *136*, 16176−16184.

(25) (a) Yang, D.; Yang, Q.; Yang, L.; Luo, Q.; Huang, Y.; Lu, Z.; Zhao, S. Novel High Performance Asymmetrical Squaraines for Small Molecule Organic Solar Cells with a High Open Circuit Voltage of 1.12 V. *Chem. Commun.* **2013**, *49*, 10465−310467. (b) Rao, G. H.; Venkateswararao, A.; Giribabu, L.; Han, L.; Bedja, I.; Gupta, R. K.; Islam, A.; Singh, S. P. Near-Infrared Squaraine Co-Sensitizer for High-Efficiency Dye-Sensitized Solar Cells. *Phys. Chem. Chem. Phys.* **2016**, *18*, 14279−14285.

(26) Cox, J. R.; Müller, P.; Swager, T. M. Interrupted Energy Transfer: Highly Selective Detection of Cyclic Ketones in the Vapor Phase. *J. Am. Chem. Soc.* **2011**, *133*, 12910−12913.

(27) Thomas, J.; Sherman, D. B.; Amiss, T. J.; Andaluz, S. A.; Pitner, J. B. Synthesis and Biosensor Performance of a Near-IR Thiol-Reactive Fluorophore Based on Benzothiazolium Squaraine. *Bioconjugate Chem.* **2007**, *18*, 1841−1846.

(28) Chen, C.-T.; Marder, S. R.; Cheng, L.-T. Syntheses and Linear and Nonlinear Optical Properties of Unsymmetrical Squaraines with Extended Conjugation. *J. Am. Chem. Soc.* **1994**, *116*, 3117−3118.

(29) Smits, E. C. P.; Setayesh, S.; Anthopoulos, T. D.; Buechel, M.; Nijssen, W.; Coehoorn, R.; Blom, P. W. M.; de Boer, B.; de Leeuw, D. M. Near-Infrared Light-Emitting Ambipolar Organic Field-Effect Transistors. *Adv. Mater.* **2007**, *19*, 734−738.

(30) Wöbkenberg, P. H.; Labram, J. G.; Swiecicki, J.-M.; Parkhomenko, K.; Sredojevic, D.; Gisselbrecht, J.-P.; de Leeuw, D. M.; Bradley, D. D. C.; Djukic, J.-P.; Anthopoulos, T. D. Ambipolar Organic Transistors and Near-Infrared Phototransistors Based on a Solution-Processable Squarilium Dye. *J. Mater. Chem.* **2010**, *20*, 3673−3680.

(31) Sun, Q.; Dong, G.; Zhao, H.; Qiao, J.; Liu, X.; Duan, L.; Wang, L.; Qiu, Y. Modulated Intermolecular Electrostatic Interaction and Morphology Transition in Squarylium Dyes Based Organic Field-effect Transistors. *Org. Electron.* **2011**, *12*, 1674−1682.

(32) Gsänger, M.; Kirchner, E.; Stolte, M.; Burschka, C.; Stepanenko, V.; Pflaum, J.; Würthner, F. High-Performance Organic Thin-Film Transistors of J-Stacked Squaraine Dyes. *J. Am. Chem. Soc.* **2014**, *136*, 2351−2362.

(33) Paternò, G. M.; Moretti, L.; Barker, A. J.; D'Andrea, C.; Luzio, A.; Barbero, N.; Galliano, S.; Barolo, C.; Lanzani, G.; Scotognella, F. Near-Infrared Emitting Single Squaraine Dye Aggregates with Large Stokes Shifts. *J. Mater. Chem. C* **2017**, *5*, 7732−7738.

(34) Würthner, F.; Kaiser, T. E.; Saha-Möller, C. R. J-Aggregates: From Serendipitous Discovery to Supramolecular Engineering of Functional Dye Materials. *Angew. Chem., Int. Ed.* **2011**, *50*, 3376−3410.

(35) Marchena, M. J.; de Miguel, G.; Cohen, B.; Organero, J. A.; Pandey, S.; Hayase, S.; Douhal, A. Real-Time Photodynamics of Squaraine-Based Dye-Sensitized Solar Cells with Iodide and Cobalt Electrolytes. *J. Phys. Chem. C* **2013**, *117*, 11906−11919.

(36) Vandewal, K.; Benduhn, J.; Nikolis, V. C. How to Determine Optical Gaps and Voltage Losses in Organic Photovoltaic Materials. *Sustainable Energy Fuels* **2018**, *2*, 538−544.

(37) Pavlishchuk, V. V.; Addison, A. W. Conversion Constants for Redox Potentials Measured Versus Different Reference Electrodes in Acetonitrile Solutions at 25 °C. *Inorg. Chim. Acta* **2000**, *298*, 97−102.

(38) Pandey, S. S.; Morimoto, T.; Fujikawa, N.; Hayase, S. Combined Theoretical and Experimental Approaches for Development of Squaraine Dyes with Small Energy Barrier for Electron Injection. *Sol. Energy Mater. Sol. Cells* **2017**, *159*, 625−632.

(39) http://www.pulsedpower.net/Info/workfunctions.htm.

(40) Frisch, M. J.; Trucks, G. W.; Schlegel, H. B.; Scuseria, G. E.; Robb, M. A.; Cheeseman, J. R.; Scalmani, G.; Barone, V.; Mennucci, B.; Petersson, G. A.; Nakatsuji, H.; Caricato, M.; Li, X.; Hratchian, H. P.; Izmaylov, A. F.; Bloino, J.; Zheng, G.; Sonnenberg, J. L.; Hada, M.; Ehara, M.; Toyota, K.; Fukuda, R.; Hasegawa, J.; Ishida, M.; Nakajima, T.; Honda, Y.; Kitao, O.; Nakai, H.; Vreven, T.; Montgomery, J. A., Jr.; Peralta, J. E.; Ogliaro, F.; Bearpark, M.; Heyd, J. J.; Brothers, E.; Kudin, K. N.; Staroverov, V. N.; Kobayashi, R.; Normand, J.; Raghavachari, K.; Rendell, A.; Burant, J. C.; Iyengar, S. S.; Tomasi, J.; Cossi, M.; Rega, N.; Millam, J. M.; Klene, M.; Knox, J. E.; Cross, J. B.; Bakken, V.; Adamo, C.; Jaramillo, J.; Gomperts, R.; Stratmann, R. E.; Yazyev, O.; Austin, A. J.; Cammi, R.; Pomelli, C.; Ochterski, J. W.; Martin, R. L.; Morokuma, K.; Zakrzewski, V. G.; Voth, G. A.; Salvador, P.; Dannenberg, J. J.; Dapprich, S.; Daniels, A. D.; Farkas, O.; Foresman, J. B.; Ortiz, J. V.; Cioslowski, J.; Fox, D. J. *Gaussian 09*, revision A.02; Gaussian Inc.: Wallingford, CT, 2009.

(41) Yamaguchi, Y.; Pandey, S. S.; Fujikawa, N.; Ogomi, Y.; Hayase, S. A Combined Theoretical and Experimental Approaches Towards Designing NIR Dyes for Dye-Sensitized Solar Cells. *J. Eng. Sci. Technol.* **2014**, 51−65.

(42) Pradhan, A.; Morimoto, T.; Saikiran, M.; Kapil, G.; Hayase, S.; Pandey, S. S. Investigation of the Minimum Driving Force for Dye Regeneration Utilizing Model Squaraine Dyes for Dye-Sensitized Solar Cells. *J. Mater. Chem. A* **2017**, *5*, 22672−22682.

(43) Kuster, S.; Geiger, T. Strategies and Investigations on Bridging Squaraine Dye Units. *Dyes Pigm.* **2012**, *95*, 657−670.